Noel, J. G., Hui, D. Y., Blankenship, D. T., & Harmony, J. A. K. (1981) *Biochim. Biophys. Acta 665*, 519–530.
Prendergast, F. G., Hangland, R. P., & Callahan, P. J. (1981) *Biochemistry 20*, 7333–7338.
Ranganathan, S., Jackson, R. L., & Harmony, J. A. K. (1982a) *Atherosclerosis (Shannon, Irel.) 44*, 261–273.
Ranganathan, S., Harmony, J. A. K., & Jackson, R. L. (1982b) *Biochem. Biophys. Res. Commun. 107*, 217–224.
Scatchard, G. (1949) *Ann. N.Y. Acad. Sci. 51*, 660–672.
Sklar, L. A., Doody, M. C., Gotto, A. M., Jr., & Pownall, H. J. (1980) *Biochemistry 19*, 1294–1301.
The Lipid Research Clinics Coronary Primary Prevention Trial Results (1984) *JAMA, J. Am. Med. Assoc. 251*, 351–374.
Thompson, R. E., Spivey, H. O., & Katz, A. J. (1976) *Biochemistry 15*, 862–867.
Tikkanen, M., & Schonfeld, G. (1985) *Biochem. Biophys. Res. Commun. 126*, 773–777.
Triplett, R. B., & Fisher, W. R. (1978) *J. Lipid Res. 19*, 478–488.
Weech, P. K., Chapman, M. J., Mills, G. L., & Goldstein, S. (1981) *Eur. J. Biochem. 120*, 191–196.
Yamamoto, M., Ranganathan, S., & Kottke, B. A. (1985) *J. Biol. Chem. 260*, 8509–8513.

Structural Changes in Membranes of Large Unilamellar Vesicles after Binding of Sodium Cholate†

Rolf Schubert,*,‡ Klaus Beyer,§ Hartwig Wolburg,∥ and Karl-Heinz Schmidt‡

Chirurgische Klinik and Pathologisches Institut, Universität Tübingen, 7400 Tübingen, FRG, and Institut für Physikalische Biochemie, Universität München, 8000 München 2, FRG

Received November 22, 1985; Revised Manuscript Received April 14, 1986

ABSTRACT: The interaction of the bile salt cholate with unilamellar vesicles was studied. At low cholate content, equilibrium binding measurements with egg yolk lecithin membranes suggest that cholate binds to the outer vesicle leaflet. At increasing concentrations, further bile salt binding to the membrane is hampered. Before the onset of membrane solubilization, diphenylhexatriene fluorescence anisotropy decreases to a shallow minimum. It then increases to the initial value in the cholate concentration range of membrane solubilization. At still higher cholate concentrations, a drop in fluorescence anisotropy indicates the transformation of mixed disk micelles into spherical micelles. Perturbation of the vesicle membranes at molar ratios of bound cholate/lecithin exceeding 0.15 leads to a transient release of oligosaccharides from intravesicular space. The cholate concentrations required to induce the release depend on the size of the entrapped sugars. Cholesterol stabilizes the membrane, whereas, in spite of enhanced membrane order, sphingomyelin destabilizes the membrane against cholate. Freeze–fracture electron microscopy and phosphorus-31 nuclear magnetic resonance (^{31}P NMR) also reflect a change in membrane structure at maximal cholate binding to the vesicles. In ^{31}P NMR spectra, superimposed on the anisotropic line typically found in phospholipid bilayers, an isotropic peak was found. This signal is most probably due to the formation of smaller vesicles after addition of cholate. The results were discussed with respect to bile salt/membrane interactions in the liver cell. It is concluded that vesicular bile salt transport in the cytoplasm is unlikely and that cholate binding is restricted to the outer leaflet of the canalicular part of the plasma membrane.

Bile acids play an important role in the absorption of dietary lipids from the intestine. De novo synthesis from cholesterol and conjugation in the liver cell are well understood. Reabsorption into the liver during enterohepatic circulation seems to be due to carrier-mediated cotransport with sodium through the sinusoidal part of the plasma membrane of the liver cell [for reviews, see Matern & Gerok (1979) and Blitzer & Boyer (1982)].

The mechanism of bile salt excretion, however, remains controversial. On the one hand, a carrier-mediated transport through the bile canalicular part of the liver cell plasma membrane cannot be excluded (Erlinger, 1981). On the other, electron microscopic studies under conditions of enhanced bile salt excretion (Boyer et al., 1978; Jones et al., 1979) suggested transport of bile salts in Golgi vesicles and exocytosis across the canalicular membrane.

For further elucidation of the mechanisms of bile salt transport in the liver cell and their interaction with the canalicular membrane, we investigated the interaction of cholate with unilamellar vesicles. The structure of lipid/bile acid mixed micelles has been studied repeatedly (Small, 1967; Mazer et al., 1976; Müller, 1981). In our opinion, unilamellar vesicles are better suited as a cellular membrane model than either mixed micelles or multibilayers when the effects of asymmetric bile acid uptake are to be studied.

Materials and Methods

Vesicle Preparation. Large unilamellar vesicles of homogeneous size were prepared by using the method of fast and controlled dialysis of mixed detergent/lipid micelles (Milsmann, 1978). Bile salts, cholesterol, lecithin from fresh egg yolk, and sphingomyelin from egg yolk were purchased from Sigma Chemical Co., St. Louis, MO.

† This work was supported by grants from the Deutsche Forschungsgemeinschaft (WO 215/7-1 and Schm 579/2-3).
‡ Chirurgische Klinik, Universität Tübingen.
§ Institut für Physikalische Biochemie, Universität München.
∥ Pathologisches Institut, Universität Tübingen.

0006-2960/86/0425-5263$01.50/0

Cholesterol and also sodium cholate were recrystallized twice from methanol before use. Lipids and, if necessary, [^{14}C]-dipalmitoylphosphatidylcholine ([^{14}C]DPPC)[1] (NEN Chemicals, Dreieich, FRG), were dissolved together with cholate in methanol. Solvent was removed completely under reduced pressure, and dry lipid/detergent mixture was dissolved in phosphate buffer (10 mmol/L phosphate, 150 mmol/L NaCl, pH adjusted to 7.35) to yield a final lipid concentration of 17 mmol/L and a lipid:detergent ratio of 0.6 mol/mol. The mixed micelle solution was dialyzed for at least 24 h at room temperature against a continuous flow of phosphate buffer, using a commercially available dialysis apparatus (LIPOPREP, Diachema, Langnau, Switzerland) and a highly permeable dialysis membrane with a cutoff of 10000 daltons (Diachema).

Vesicles formed from pure egg yolk lecithin (EYL), EYL/sphingomyelin (7:3 mol/mol), or EYL/cholesterol (7:3 mol/mol) were homogeneous in size with a mean diameter of 70, 120, or 100 nm, respectively, as determined by laser autocorrelation spectrometry (NANOSIZER, Coulter Electronics Ltd., Harpenden, U.K.). The vesicles appeared unilamellar on electron micrographs of freeze–fracture replicas.

To avoid isotropic ^{31}P NMR signals due to vesicle rotation, vesicles with a diameter greater than 200 nm were prepared. For this purpose, EYL was mixed with *n*-octyl β-D-glucopyranoside at a molar ratio of 0.2. The mixed micelle solution was prepared as described above, except that MOPS was used as buffer substance. Dialysis membranes with a cutoff of 5000 daltons (Diachema) were used to obtain homogeneous liposomes with a mean diameter of 200 nm. The turbidity of the vesicle suspension was diminished by short vortexing, thus indicating reversible aggregation of the slowly tumbling neutral vesicles.

After fractionation on Sepharose 2B-CL (Pharmacia Fine Chemicals AB, Uppsala, Sweden), liposomes with a diameter greater than 200 nm were collected and pelleted by ultracentrifugation (90 min, 140000*g*). Pellets were resuspended in MOPS buffer containing D_2O (Riedel-deHaen AG, Seelze, FRG) instead of water to yield a final lipid concentration of 50 mmol/L. Electron microscopy showed predominantly unilamellar vesicles with little contamination of oligolamellar liposomes.

Entrapping of tritium-labeled raffinose, inulin, or dextran (NEN) was performed by adding radioactive markers to the buffer used to dissolve the dry lipid/detergent mixture and to the dialysis buffer used until vesicle formation was completed [for details, see Schubert et al. (1983)].

Equilibrium Binding Studies. Binding equilibria of EYL vesicles (mean diameter 80 nm) and cholate were studied with cholate concentrations varying from 20 μmol/L to 30 mmol/L. Lecithin (total concentration 750 μmol/L) was labeled with [^{14}C]DPPC and cholate with [^{3}H]cholic acid (NEN). The pH of all incubations was 7.35.

Up to a total cholate concentration of 4.5 mmol/L, 2 mL of vesicle suspensions in different cholate concentrations was ultracentrifuged in polycarbonate tubes (140000*g*, 210 min, 25 °C; Beckman L5-75, rotor Ti 50.3). Free cholate concentrations were determined in the supernatants.

At total cholate concentrations >4.5 mmol/L, i.e., in the presence of mixed micelles, binding equilibria were studied by equilibrium dialysis at room temperature using highly permeable cellulose membranes (cutoff 10000 daltons, Diachema). Dialysis chambers were rotated for 4 h in a commercially available apparatus (Diachema, Switzerland).

Binding equilibria between cholate up to concentrations of 20 mmol/L and highly concentrated EYL vesicle membranes (45 mmol/L) of 220-nm diameter were determined by analyzing the free cholate in the supernatant after pelleting of 200 μL of the suspension (see below).

Determination of Vesicle Stability. Cholate-dependent vesicle stability was determined by ultracentrifugation or gel chromatography. Two milliliters of suspensions containing 70-nm vesicles of a low lecithin concentration (750 μmol/L) and varying cholate concentrations was ultracentrifuged (140000*g*, 210 min, 25 °C). In the supernatants, release of radioactively labeled carbohydrates and lecithin from vesicles was determined. The observation that during cholate-induced membrane solubilization the appearance of [^{14}C]DPPC in the supernatants exactly coincides with a decrease in turbidity furnishes evidence that the radioactive lecithin mimicks the behavior of EYL. Gel chromatography of the same vesicle/cholate mixtures was performed on Sepharose 4B-CL (Pharmacia) to determine released inulin or solubilized lecithin.

The stability of 220-nm vesicle suspensions containing 45 mmol/L EYL against cholate was checked by determining [^{14}C]DPPC in the supernatant after pelleting (180000*g*, 4 h) of 200-μL suspensions (Airfuge, rotor 30° A-100, Beckman Instruments) and by column chromatography on Sepharose 2B-CL.

DPH Fluorescence Anisotropy Measurements. DPH (Sigma) was suspended in phosphate buffer by tip sonication (2 min, 15 W, Branson Co., Danbury, CN) and mixed with the vesicle suspension to yield a molar lipid:DPH ratio of 400:1. The mixture was incubated for 12 h at 30 °C in the absence of light. Thereafter, fluorescence leveled off. Compared to the commonly used method in which DPH is added in tetrahydrofuran solution, this procedure avoids any influence of organic solvents on the cholate/liposome interaction.

Fifty microliters of DPH-labeled vesicle suspensions was mixed with 1.65 mL of cholate solution in phosphate buffer. Final cholate concentration varied from 0 to 20 mmol/L. The lipid concentration was 150 μmol/L.

Steady-state anisotropy measurements were performed with an MPF-3 fluorescence spectrometer (Perkin-Elmer, Norwalk, CN) using polarizing filters in the excitation and emission light paths. Samples were excited at 366 nm. $I_\parallel$ and $I_\perp$, fluorescence intensities parallel and perpendicular to the excitation beam, respectively, were recorded at 430 nm. An additional cutoff filter of 390 nm reduced stray light. Fluorescence intensities were corrected for scattered light of unlabeled vesicle suspensions. Light-scattering contribution to total $I_\parallel$ was less than 2%.

To reduce fluorescence shifts caused by photoisomerization of DPH (Shinitzky & Barenholz, 1974) and increase of sample temperature by irradiation, exposure periods to excitation were no longer than 5 s. Temperature was held constant at 26 ± 0.5 °C, as recorded by a thermistor probe (Hellma GmbH, Müllheim, FRG) in the measured sample. Fluorescence measurements were performed 10 min after vesicles were mixed with detergent.

The steady-state fluorescence anisotropy, r_s, was determined as

$$r_s = (I_\parallel - I_\perp)/(I_\parallel + 2I_\perp)$$

^{31}P NMR. ^{31}P NMR spectra were obtained at 25 °C on a Bruker SXP4-100 spectrometer operating at a ^{31}P frequency of 36.4 MHz. Broad-band decoupling was applied at a power

[1] Abbreviations: cLPM, canalicular part of the liver cell plasma membrane; ^{2}H NMR, deuterium nuclear magnetic resonance; ^{31}P NMR, phosphorus-31 nuclear magnetic resonance; [^{14}C]DPPC, [^{14}C]dipalmitoylphosphatidylcholine; DPH, 1,6-diphenyl-1,3,5-hexatriene; EYL, egg yolk lecithin; MOPS, 3-(*N*-morpholino)propanesulfonic acid.

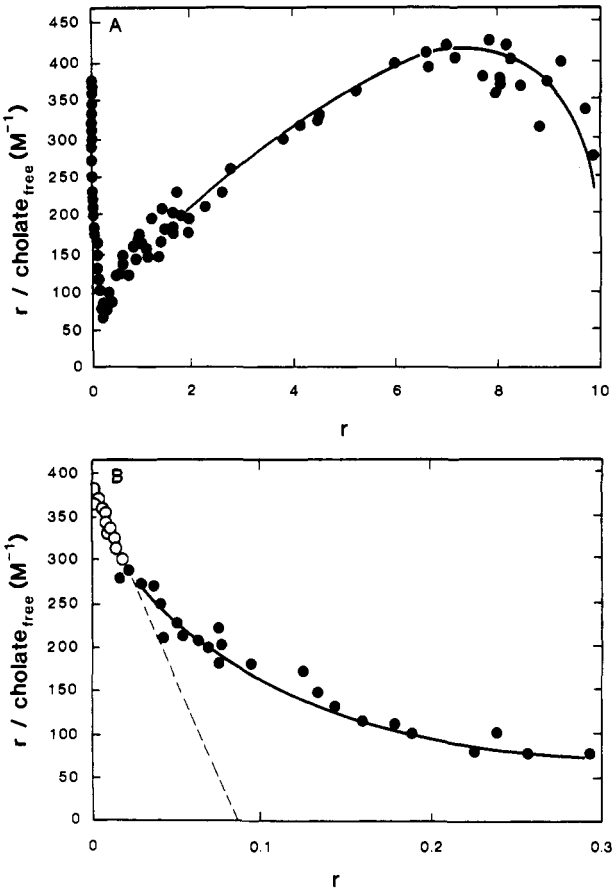

FIGURE 1: Scatchard plots of cholate/EYL binding equilibria (mean vesicle diameter, 80 nm; total EYL concentration, 750 μmol/L). (A) Cholate concentration range up to 25 mmol/L. (B) Cholate concentration range up to 4 mmol/L. No EYL solubilization was detectable in this concentration range. Open circles represent cholate concentrations up to 200 μmol/L used to calculate initial binding of cholate to EYL (see text).

output of approximately 0.15 mT. The pulse repetition rate was 1 s^{-1} and pulse angle, ≈70°.

Electron Microscopy. Vesicle suspensions were drawn up with a micropipet, mounted directly into the central hole (1 mm in diameter) of a pair of gold specimen holders, shock-frozen in nitrogen slush (−210 °C), and transferred to a Balzers freeze–fracturing BAF 400 D apparatus equipped with an oscillating quartz (QSG 301). The specimens were fractured at about 5×10^{-6} mbar and −150 °C and then shadowed with platinum/carbon (45 °C; 2 nm) and carbon (20 nm) for replica stabilization. To avoid any condensation at the fracture faces, shadowing was started before fracturing. Replicas were directly cleaned several times in distilled water. Our studies showed that treatment with sodium hypochlorite, commonly used in cleaning replicas of biological tissues, is unnecessary in processing liposome replicas. Replicas were mounted on pioloform-coated copper grids and observed in a Siemens Elmiscop 102 electron microscope.

RESULTS

Equilibrium Binding of Cholate to Lecithin Vesicles. The binding of [^{3}H]cholate to large unilamellar lecithin vesicles was determined by ultracentrifugation or by equilibrium dialysis (see Materials and Methods). Figure 1A shows a Scatchard plot for a wide range of cholate concentrations comprising the region in which the vesicle membranes are completely transformed into mixed micelles. Figure 1B represents an enlarged version of Figure 1A for very low cholate additions.

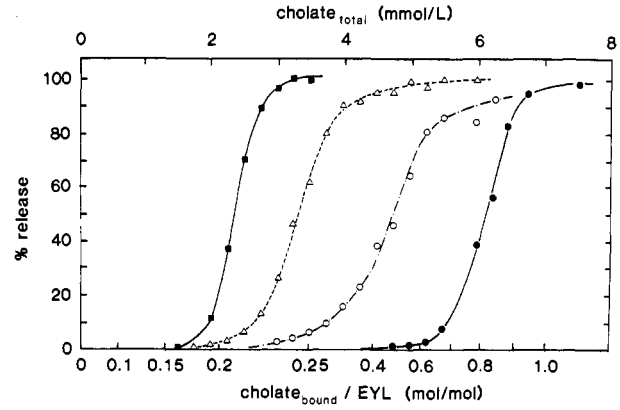

FIGURE 2: Carbohydrate and lecithin release from EYL vesicles (mean vesicle diameter, 70 nm; total EYL concentration, 750 μmol/L). (□) [^{3}H]Raffinose (M_r 594); (△) [^{3}H]inulin (M_r 5000); (○) [^{3}H]dextran (M_r 70 000); (●) [^{14}C]DPPC.

In Figure 1B, i.e., at low molar ratio (r) of bound cholate to total lecithin, the plot is biphasic. Up to $r = 0.025$, the Scatchard relationship is essentially linear. An apparent maximal binding constant $K_a = 4800\ M^{-1}$ may be calculated from the slope of this initial part. To overcome the inaccuracy in extrapolation of the initial part of the Scatchard graph to the abscissa (Klotz, 1982), the number of binding sites (n) was determined with a distribution-free computer method (Crabbe, 1985). n was calculated as 0.087. Assuming that cholate binds exclusively to the outer leaflet, the calculated maximal binding would correspond to about six lecithin molecules associated with one cholate molecule. The deviation from linearity and the reduced slope at $r > 0.025$ in Figure 1B suggest that binding of additional cholate to the vesicle membrane is hampered.

At $r > 0.3$, after ultracentrifugation radioactively labeled lecithin appears in the supernatant, thus indicating solubilization of the vesicle membrane. Figure 1A shows the total concentration range in which mixed micelles are formed. The shape of the curve above $r = 0.3$ is typical for positively cooperative binding processes. The maximal cholate:lecithin ratio in the mixed micelles is approximately 10 mol/mol as obtained by extrapolation of the plot at high r values.

Stability of Vesicles against Cholate. The gradual release of carbohydrates from preloaded vesicles at addition of increasing amounts of cholate is shown in Figure 2. The cholate concentration required for half-maximal release increases with the molecular weight of the untrapped carbohydrate molecules. Interestingly enough, carbohydrate release occurs well below the cholate concentration necessary to form mixed micelles, as indicated by the appearance of [^{14}C]lecithin in the supernatant.

Release curves essentially the same as those in Figure 2 were obtained when vesicles loaded with inulin were incubated for 24 h with increasing amounts of cholate prior to centrifugation (data not presented). This observation tends to refute a continuous diffusion of entrapped carbohydrate across the vesicle membrane and tends to support the formation of transient holes.

The total cholate concentration necessary for half-maximal vesicle solubilization is lowered by approximately 1.5 mmol/L when the membranes contain 30 mol % sphingomyelin; 30 mol % cholesterol, however, leads to a solubilization threshold increase of 3 mmol/L. Almost the same relative shifts in effective cholate concentration are necessary to induce inulin release (experiments not presented). Cholesterol clearly stabilizes the membrane against the action of cholate, whereas

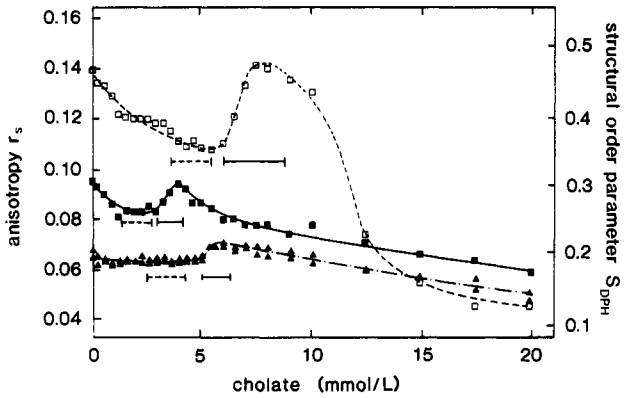

FIGURE 3: Cholate-dependent steady-state fluorescence anisotropy, r_s, of DPH and structure order parameter, S_{DPH}, in vesicle membranes and mixed micelles. (▲) Pure EYL; (■) EYL/sphingomyelin 7:3 (mol/mol); (□) EYL/cholesterol 7:3 (mol/mol); (dashed horizontal bars) release of inulin; (solid horizontal bars) vesicle solubilization.

sphingomyelin has a destabilizing effect.

It may be argued that mechanical stress during ultracentrifugation leads in and of itself to loss of entrapped carbohydrate molecules from vesicles, partially destabilized by membrane-bound cholate. Consequently, in a parallel experiment, vesicles were separated from released inulin on a Sepharose 4B-CL column. The cholate concentration resulting in half-maximal carbohydrate release was indeed approximately 25% higher than that in the centrifugation experiments. Membrane solubilization, however, was detected in the same range of cholate concentrations as depicted in Figure 2 (data not presented).

In highly concentrated suspensions (45 mmol of EYL/L) as used in ^{31}P NMR experiments (see below), no membrane solubilization was detectable up to a molar ratio r of bound cholate to lecithin of 0.28. In contrast to the diluted samples, however, column chromatography on Sepharose 2B-CL and autocorrelation spectrometry showed that the addition of cholate led to the formation of smaller vesicles. At $r = 0.12$, approximately 5% of the total lipid was found in vesicles smaller than 190 nm with an average diameter of 100 nm. At $r = 0.28$, a yet larger portion (about 40%) of the phospholipid was detected in vesicles ranging from 130 to 190 nm.

Fluorescence Anisotropy Measurements. The internal order in various membrane/cholate mixtures was studied by using diphenylhexatriene (DPH) as a fluorescence probe. Figure 3 shows the change in steady-state fluorescence anisotropy, r_s, at the addition of increasing cholate concentrations to DPH-containing vesicles.

The ranges of cholate concentrations leading to inulin release and membrane solubilization, as determined by the centrifugation method (see above), are indicated in Figure 3 (see also Figure 2). Structural order parameters, S_{DPH}, were calculated according to van Blitterswijk et al. (1981).

Binding of cholate to lecithin vesicles and to vesicles containing 30 mol % cholesterol or 30 mol % sphingomyelin leads to considerably different initial r_s values. Changes in r_s at cholate addition, however, are similar in the different vesicle preparations (Figure 3). Shallow minima of r_s occur in the concentration region of inulin permeability. After complete solubilization, r_s attains maximal values which are nearly identical with the anisotropies observed in the absence of cholate.

At very high cholate:membrane lipid ratios, r_s obviously approaches lower limiting values between 0.045 and 0.06.

^{31}P NMR. The perturbation in membrane architecture caused by the binding of cholate was studied by ^{31}P NMR.

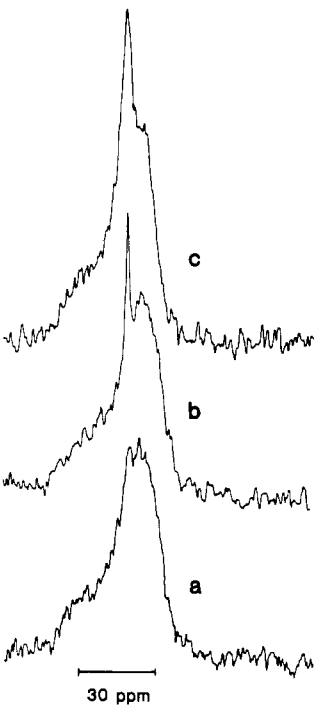

FIGURE 4: ^{31}P NMR spectra of large EYL vesicles (mean diameter, 220 nm) at increasing cholate content. EYL concentration in all samples was 45 mmol/L. (a) Cholate-free vesicles. (b) Molar ratio, r, of bound cholate/total EYL = 0.12. (c) $r = 0.28$. Experimental line broadening, 18.6 Hz. The line widths of the narrow peaks in (b) and (c) are about 20 and 110 Hz, respectively.

In large (>200 nm) vesicles, ^{31}P NMR line shape provides information on the internal structure of the phospholipid aggregate. In small unilamellar vesicles, this information is lost due to motional averaging of the intrinsic ^{31}P chemical shift anisotropy (Burnell et al., 1980). Large unilamellar vesicles with an average diameter of 220 nm, therefore, were prepared for ^{31}P NMR experiments.

The bilayer structure in these vesicles is clearly reflected in the anisotropic envelope of the ^{31}P signal (see Figure 4a). In comparison to the anisotropy value typically found in multilamellar liposomes (40 ppm), the chemical shift anisotropy (33 ppm) is slightly reduced. When cholate is added to yield a bound cholate:EYL ratio of 0.12 mol/mol, a narrow peak indicative of isotropic phospholipid motion appears in the spectrum (Figure 4b). It is important to note that no phospholipid solubilization, i.e., formation of mixed micelles, was detected at this cholate concentration (cf. Figure 2) and that the vesicles also remained impermeable for carbohydrate molecules of low molecular weight (cf. Figure 2).

Further addition of cholate at nonsolubilizing concentrations leads to a considerable broadening of the superimposed isotropic peak without the anisotropic portion of the spectrum being affected (Figure 4c). Increasing the cholate concentration ultimately results in a single narrow signal about 10 Hz in line width due to the formation of mixed micelles (not presented).

Electron Microscopy. Structural changes induced by the addition of cholate to differently sized vesicles were studied by freeze–fracturing electron microscopy (Figure 5). Before cholate addition, the vesicles show smooth fracture faces (not presented). Both preparations contain almost exclusively unilamellar vesicles with an average diameter of 70 and 220 nm, respectively.

No effect was detectable on the micrographs after addition of cholate up to a molar ratio of 0.12 bound cholate/lecithin (not presented). After further addition of cholate, however,

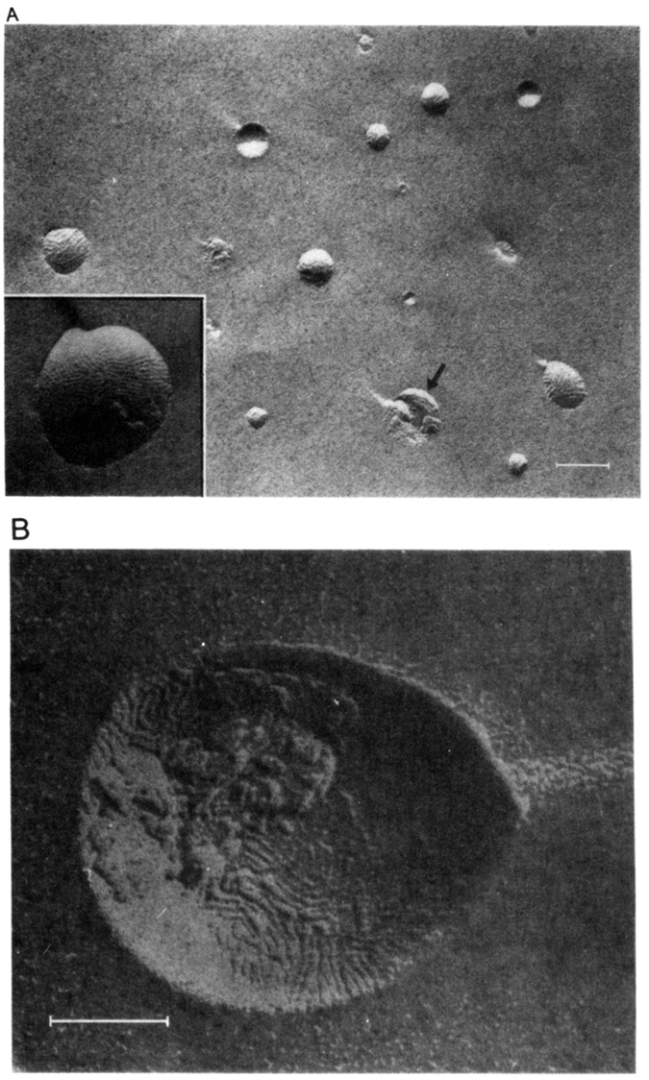

FIGURE 5: Freeze–fracture replicas of EYL vesicles. Bars represent 100 nm. (A) 70-nm vesicles after addition of cholate to yield a bound cholate:EYL molar ratio of $r = 0.28$. Note membrane ripples with repeat distance of 8 nm. Fusion leads to cochleate-like structures (arrow) and multilamellar liposomes (see insert). (B) 220-nm vesicles after cholate addition, $r = 0.28$. Membrane ripples are the same size as in (a).

a rippled structure appeared on the freeze–fracture faces (Figure 5A,B).

Multilamellar aggregates are found in both vesicle samples after cholate treatment. The multilamellar liposomes appearing in the small vesicle preparation are similar in size to the multilamellar structures originating from the large vesicles. Obviously, cholate induces a certain amount of vesicle fusion. It should be noted that the ripple structure is observed in both unilamellar and multilamellar vesicles. The ripples, therefore, are not the consequence of membrane fusion, but they may well represent an early stage of the fusion event.

In the electron micrographs, another intriguing feature is the spirallike structures (see Figure 5A), which are very similar to the "cochleate cylinders" occurring in phosphatidylserine membranes after the addition of calcium (Papahadjopoulos et al., 1975).

Discussion

Our study deals with the interaction of the bile salt cholate with unilamellar vesicles. Large unilamellar vesicles provide an excellent model for the cell membrane bilayer. In the first stage of cholate binding to the phospholipid membrane, heterogeneous distribution of the bile salt among the bilayer leaflets can be assumed. Physical effects due to this heterogeneity in cholate distribution can only be adequately studied in unilamellar vesicles.

On the basis of NMR experiments, Ulmius et al. (1982) recently concluded that bound cholate molecules are very probably placed flat on the membrane surface rather than intercalated into the membrane between the phospholipid molecules. Following this reasoning, the equilibrium binding data in our study (see Figure 1) suggest the formation of EYL/cholate aggregates in the outer layer of the vesicle membrane with six molecules of lecithin per cholate monomer. The Scatchard plot indicates that cholate binding beyond a limiting molar ratio of bound cholate/EYL of 0.025 (i.e., 0.05 in the outer monolayer) is hampered.

Specifically deuterated deoxycholate and chenodeoxycholate, however, were found to be incorporated perpendicularly with respect to the surface of a lecithin bilayer membrane (Saito et al., 1983). It, therefore, may be assumed that these bile acids form dimers when they are intercalated in the phospholipid membrane and, thereby, avoid contact between the phospholipid fatty acid chains and the bile salt hydroxy groups. Equilibrium binding studies with chenodeoxycholate yielded an initial extrapolated bile salt:EYL binding ratio of 0.17 mol/mol (R. Schubert, unpublished results). This then suggests that bile salt dimers are inserted in the outer monolayer and surrounded by six molecules of phospholipid. The mode of bile salt/membrane interaction, therefore, seems to depend to a great extent on the number of hydroxy groups on the hydrophilic hemisphere of the bile salt molecule.

The cholate-induced decrease in the membrane order parameter, as derived from fluorescence anisotropy measurements, generally agrees with the earlier finding that the presence of this bile salt leads to a decreased deuterium NMR order parameter, S_{CD} (Ulmius et al., 1982), of fatty acid CD_2 segments in a specifically deuterated lecithin. The ^2H NMR data, however, were obtained in liquid-crystalline mixtures at rather low water content. In addition, the decrease in membrane order was only observed at elevated cholate:lecithin ratios.

Nevertheless, the tentative conclusions drawn by Ulmius et al. (1982), i.e., that cholate binding leads to larger separation of the lecithin molecules and, thereby, to an increase in configurational space in the fatty acyl chains, may also apply in the case of dilute vesicle suspensions. The observation that the initial decrease in membrane order is strikingly more pronounced in the presence of cholesterol (Figure 3) suggests that cholate binding to a large extent overcomes the well-known "condensing effect" of cholesterol (Demel & de Kruijff, 1976).

An obvious consequence of the perturbation induced by cholate is the release of entrapped carbohydrates. In titration experiments, the onset of carbohydrate release is not accompanied by the formation of mixed phospholipid/cholate micelles (see Figure 2). The release observed at low cholate concentrations, therefore, is not due to vesicle solubilization. Moreover, the observation that the colate concentration required for release increases with the molecular weight of the entrapped carbohydrate molecules does not support a partial micellization of the phospholipid vesicles.

The gradual release of hydrophilic molecules from the intravesicular space may be due to the formation of transient pores. Increasing cholate concentration could result in an increasing average size of these intramembrane pores. Our experiments, however, show that the carbohydrate efflux ceases

shortly after addition of cholate, thus suggesting rapid resealing of the bile salt induced intramembrane pores. One suggested theory of pore formation is that the free energy of the bilayer edges is lowered by foreign molecules (Kashchiev & Exerowa, 1983). In the present case, this mechanism is only operative immediately after bile salt uptake. Redistribution of bile salt molecules may then lead to rapid membrane stabilization.

Interestingly enough, carbohydrate release occurs in that range of cholate:EYL ratios where the Scatchard plot sharply deviates from linearity (see Figure 1). In the same region, the membrane order, as derived from DPH fluorescence anisotropy, reaches a minimum, regardless of the initial anisotropy and the composition of the unperturbed membrane.

Our experiments did not substantiate the assumptions of O'Connor et al. (1985), who presumed that bile salt damage is closely related to membrane fluidity, nor Coleman et al. (1980), who traced the erythrocyte stability against bile salts to the presence of sphingomyelin. Our data, however, demonstrate that both inulin release and membrane solubilization occurred at lower bile salt concentrations than with pure EYL membranes, in spite of the enhanced order of sphingomyelin-containing membranes (see Figure 3).

The narrow ^{31}P NMR line superimposed on the broad anisotropic "bilayer signal" is most probably due to the formation of smaller vesicles as revealed by gel chromatography and autocorrelation spectrometry. Even though such vesicles were not detectable in electron micrographs, they may have been formed in the highly concentrated suspensions used for NMR experiments. The increasing intensity of the isotropic signal with cholate concentration is in line with the increasing total amount of smaller vesicles. Also the increase in line width seems to reflect the broader size distribution found after gel chromatography. It cannot be excluded, however, that the rippled intramembrane structures observed in freeze–fracture electron micrographs (cf. Figure 5) may contribute to the narrow ^{31}P NMR signal. The ripples probably consist of highly curved membrane regions in which rapid phospholipid diffusion may lead to an averaging of the ^{31}P chemical shift anisotropy (de Kruijff et al., 1979).

One intriguing finding was the increase in DPH fluorescence anisotropy at membrane solubilization (Figure 3). It suggests a restoration of the internal order in the solubilized membrane fragments. The level of the order parameter, as derived from the fluorescence data, is apparently the same as in the unperturbed membrane. The mixed disk micelle model of phospholipids and bile salts suggested by Mazer et al. (1976) would explain this finding. According to this model, the mixed micelles form flat disklike membrane fragments. This model is in agreement with the results of a recent low-angle X-ray study at low bile salt:lecithin ratios (Müller, 1981). The enhanced structural order, as obtained by DPH fluorescence anisotropy, suggests that, in contrast to unsolubilized membranes at lower bile salt concentrations, the bile salt molecules in these bilayer micelles are parallel correlated to cholesterol and to the hydrophobic chains of the phospholipids.

Transformation of the mixed disk micelles into spherical micelles at bile salt:lecithin ratios between 1.5 and 2 mol/mol was detected earlier by differential scanning calorimetry (Claffey & Holzbach, 1981) and X-ray scattering (Müller, 1981). The decrease in r_s at cholate:EYL ratios greater than 1.0 indicates that the interior of the mixed disk micelle is disturbed before the transformation into a spherical micelle. The diameter of the spherical micelle of 6 nm (Müller, 1981), which corresponds to a rotational correlation time of 25 ns, and the DPH fluorescence lifetime in membranes of 11 ns (Kawato et al., 1977; Lakowicz et al., 1979) argue against the suppression of fluorescence anisotropy by micelle tumbling. Local disorder in the spherical micelles, therefore, must be assumed.

In summary, the solubilization of EYL bilayer vesicles may be pictured as follows: At low bound cholate:EYL ratios, bile salt molecules are adsorbed on the membrane surface. Through asymmetric cholate binding on one bilayer side, increasing cholate binding leads to a disordering in the hydrophobic core of the membrane. Due to steric hindrance, a portion of the bile salts suddenly folds over into the bilayer. This foldover may be accompanied by the transient formation of membrane holes. Saturation of the membrane interior with cholate dimers ultimately leads to the release of mixed disk micelles, the diameters of which increase with rising cholate content (Schubert et al., 1983). Finally, with extremely high cholate content, the mixed disk micelles transform into spherical mixed micelles and their diameter decreases.

Our results could help clarify the intracellular transport of bile salts and their interaction with the canalicular part of the liver cell plasma membrane (cLPM). Jones et al. (1979) suggested that bile salts in the liver cell are transported to the cLPM via vesicles. Our experiments tend to suggest that vesicles may be loaded up to a molar ratio of bile salt/phospholipid of 1:6. The rippled structures, as observed by electron microscopy in bile salt containing vesicle membranes (cf. Figure 5A,B), may provide the membrane attachment sites (Milier, 1980) which may lead to fusion of the vesicles with the cLPM.

Bile salt conjugating enzymes, however, were detected near the cytosolic side of the cLPM (Abberger et al., 1980). To become accessible to the conjugating enzymes, bile salts must then have released from the vesicles prior to excretion into the bile canaliculi. This finding tends to refute the excretion of bile salts via an exocytotic process. Moreover, recent studies suggest that lipid secretion involving the microtubular system (Gregory et al., 1978) and bile salt excretion (Meier et al., 1984) are independent processes.

It should be noted that, after excretion into the canaliculi, free bile salt in equilibrium with mixed micelles will bind to the cLPM. Our experiments suggest that cholesterol, but not sphingomyelin (Kremmer et al., 1976), may be considered a metabolic regulator of membrane stability against free bile salt. Moreover, membrane stability is preserved, and redistribution of bile salts into the liver cell is avoided, only as long as this binding is restricted to the outer membrane leaflet. Consequently, the observed intracellular accumulation of vesicles near the cLPM during enhanced bile salt excretion (Jones et al., 1979) is probably involved in the delivery of sufficient quantities of membrane lipids to the cLPM and the mixed micelles, rather than directly in bile salt excretion.

Registry No. DPPC, 2644-64-6; sodium cholate, 361-09-1; cholic acid, 81-25-4; cholesterol, 57-88-5; raffinose, 512-69-6; inulin, 9005-80-5; dextran, 9004-54-0.

References

Abberger, H., Bickel, U., Buscher, H. P., Fuchte, K., Gerok, W., Kramer, W., & Kurz, G. (1980) in *Bile Acids and Lipids* (Paumgartner, G., Stiel, A., & Gerok, W., Eds.) MTP Press, Lancaster, U.K.

Blitzer, L. B., & Boyer, J. L. (1982) *Gastroenterology 82*, 346.

Boyer, J. L., Itabashi, M., & Hruban, Z. (1978) in *The Liver; Third International Gstaad Symposium* (Preisig, R., & Bircher, J., Eds.) p 163, Editio Cantor, Aulendorf, FRG.

Burnell, E. E., Cullis, P. R., & de Kruijff, B. (1980) *Biochim. Biophys. Acta 603*, 563.

Claffey, W. J., & Holzbach, R. T. (1981) *Biochemistry 20*, 415.

Coleman, R., Lowe, Ph. J., & Billington, D. (1980) *Biochim. Biophys. Acta 599*, 294.
Crabbe, M. J. C. (1985) *Comput. Biol. Med. 15*, 111.
Cullis, P. R., & de Kruijff, B. (1979) *Biochim. Biophys. Acta 559*, 399.
De Kruijff, B., Verkleij, A. J., van Echteld, C. J. A., Gerritsen, W. J., Mombers, C., Noordam, P. C., & de Gier, J. (1979) *Biochim. Biophys. Acta 555*, 200.
Demel, R. A. & de Kruijff, B. (1976) *Biochim. Biophys. Acta 457*, 109.
Erlinger, S. (1981) *Hepatology (Baltimore) 1*, 352.
Gregory, D. H., Vlahcevic, Z. R., Prugh, M. F., & Swell, L. (1978) *Gastroenterology 74*, 93.
Jones, A. L., Schmucker, D. L., Mooney, J. S., Ockner, R. K. & Adler, R. D. (1979) *Lab. Invest. 40*, 512.
Kashchiev, D., & Andexerowa, D. (1983) *Biochim. Biophys. Acta 732*, 133.
Kawato, S., Kinosita, K., Jr., & Ikegami, A. (1977) *Biochemistry 16*, 2319.
Klotz, I. M. (1982) *Science (Washington, D.C.) 217*, 1247.
Kremmer, T., Wisher, M. H., & Evans, W. H. (1976) *Biochim. Biophys. Acta 455*, 655.
Lakowicz, J. R., Prendergast, F. G., & Hogen, D. (1979) *Biochemistry 18*, 508.
Matern, S., & Gerok, W. (1979) *Physiol. Biochem. Pharmacol. 85*, 126.
Mazer, N. A., Kwasnick, R. F., Carey, M. C., & Benedek, G. B. (1976) *Micellization, Solubilization, Microemulsions 1*, 383.
Meier, P. J., Gordon, E., Moseley, R., & Boyer, J. L. (1974) *Ann. N.Y. Acad. Sci. 435*, 309.
Miller, R. G. (1980) *Nature (London) 287*, 166.
Milsmann, M. H. W., Schwendener, R. A., & Weder, H.-G. (1978) *Biochim. Biophys. Acta 512*, 147.
Müller, K. (1981) *Biochemistry 20*, 404.
O'Connor, Ch. J., Wallace, R. G., Iwamoto, K., Taguchi, T., & Sunamoto, J. (1985) *Biochim. Biophys. Acta 817*, 95.
Papahadjopoulos, D., Vail, W. J., Jacobson, K., & Poste, G. (1975) *Biochim. Biophys. Acta 394*, 483.
Saito, H., Sugimoto, Y., Tabeta, R., Suzuki, S., Izumi, G., Kodama, M., Toyoshima, S., & Nagata, Ch. (1983) *J. Biochem. (Tokyo) 94*, 1877.
Schubert, R., Jaroni, H., Schölmerich, J., & Schmidt, K.-H. (1983) *Digestion 28*, 181.
Shinitzky, M., & Barenholz, Y. (1974) *J. Biol. Chem. 249*, 2652.
Small, D. M. (1967) *Gastroenterology 52*, 607.
Ulmius, J., Lindblom, G., Wennerström, H., Johansson, L. B.-A., Fontell, K., Söderman, O., & Arvidson, G. (1982) *Biochemistry 21*, 1553.
Van Blitterswijk, W. J., van Hoeven, R. P., & van der Meer, B. W. (1981) *Biochim. Biophys. Acta 644*, 323.

A 59-Kilodalton Protein Associated with Progestin, Estrogen, Androgen, and Glucocorticoid Receptors†

Ping-Kaung K. Tai,‡ Yoshiaki Maeda,§ Kiyohide Nakao,‖ Najib G. Wakim, John L. Duhring, and Lee E. Faber*
Departments of Obstetrics/Gynecology and Physiology, Medical College of Ohio, Toledo, Ohio 43699
Received December 9, 1985; Revised Manuscript Received April 23, 1986

ABSTRACT: Previous studies of the anti 8.5S progestin receptor monoclonal antibody KN 382/EC1 showed that it was specific for nontransformed progestin receptors. However, with different methods of tissue disruption and the use of protease inhibitors, we found that other nontransformed steroid receptors formed immune complexes with KN 382/EC1. Binding of the antibody to rabbit uterine estrogen, progestin, and androgen and liver glucocorticoid receptor systems was characterized by sucrose density gradient centrifugation, high-pressure liquid chromatography (HPLC), immunoadsorption, and immunoblotting. Immobilized KN 382/EC1 adsorbed both M_r 59 000 and M_r 92 000 proteins. The M_r 92 000 protein appeared to be bound to the antigenic M_r 59 000 protein, and the two proteins were present in apparently the same stoichiometric relationship in several tissues. Sodium dodecyl sulfate–polyacrylamide gel electrophoresis of immunoadsorbed material revealed appreciable amounts of both proteins in testis, stomach, lung, liver, uterus, and kidney. Only trace amounts were found in skeletal or heart muscle, and none was found in blood serum. Cleveland digestion of isolated M_r 59 000 and 92 000 proteins revealed dissimilar peptide constituents. Immunoblots of material from uterus and liver resulted in staining of the M_r 59 000 protein but not the M_r 92 000 protein. We conclude that similar antigenic determinants reside in components of several nontransformed steroid receptors and they reside on an M_r 59 000 protein. It is likely, therefore, that there are common components present in nontransformed steroid receptors.

Most steroid receptors exhibit sedimentation coefficients (Faber, 1980) that can be divided into two groups. Larger complexes (7 S and greater) are referred to as nontransformed (Puri et al., 1982), untransformed, (Reker et al., 1985), or native (Baulieu, et al., 1983) receptors. Smaller receptor forms (5.5 S or less), commonly designated activated or transformed receptors, have the well-known characteristics of binding to nuclei, DNA, chromatin, and specific isolated gene sequences (Saffran et al., 1976; Baulieu et al., 1983; Renoir & Mester, 1984; von der Ahe et al., 1985). Earlier studies suggested that the conversion of the larger to the smaller forms accompanying transformation resulted from subunit dissociation (Stancel et

† Supported in part by Grants HD-09367 and AG-02776 from the NIH.
* Author to whom correspondence should be addressed.
‡ Present address: Department of Physiology, University of Michigan Medical School, Ann Arbor, MI 48109.
§ Present address: Third Department of Internal Medicine, Osaka University School of Medicine, Osaka, Japan.
‖ Present address: First Department of Internal Medicine, Toyama Medical and Pharmaceutical University, Toyama, Japan.

0006-2960/86/0425-5269$01.50/0